Vacancies in SiC: Influence of Jahn-Teller distortions, spin effects, and crystal structure

A. Zywietz, J. Furthmüller, and F. Bechstedt
Institut für Festkörpertheorie und Theoretische Optik, Friedrich-Schiller-Universität, D-07743 Jena, Germany
(Received 21 December 1998)

We present results of *first-principles* calculations for the neutral and charged Si and C monovacancies in cubic (3C) and hexagonal (4H) SiC. The calculations are based on the density functional theory in the local-density approximation as well as local spin density approximation. Explicitly a plane-wave-supercell approach is combined with ultrasoft Vanderbilt pseudopotentials to allow converged calculations. We study the atomic structure, the energetics, and the charge- and spin-dependent vacancy states. The generation of the C-site vacancy is generally accompanied by a remarkable Jahn-Teller distortion. For the Si-site vacancy only an outward breathing relaxation occurs due to the strong localization of the C dangling bonds at the neighboring C atoms. Consequently, high-spin configurations are predicted for Si vacancies, whereas the low-spin states of C vacancies exhibit a negative-*U* behavior. In the case of hexagonal polytypes, the crystal-field splitting of the upper vacancy levels does not principally modify the properties of the vacancies. The inequivalent lattice sites, however, give rise to site-related shifts of the electronic states. [S0163-1829(99)07323-3]

I. INTRODUCTION

To a great extent the electrical and optical properties of semiconductors are governed by native defects, which also exhibit interesting physics of their own. The monovacancies in silicon carbide (SiC) are prototypical systems in this respect. In SiC the situation is markedly different from that encountered in common semiconductors like silicon. Because of the stronger chemical bonding in this hard compound, the mobility of such point defects is reduced. They are thermally stable at room temperature, and far above.[1]

Vacancies can easily be created at the atomic sites by electron, proton, or neutron bombardment.[2] They usually introduce energy levels in the fundamental energy gap and, hence, can exist in different charge states. Consequently, the vacancies influence the doping efficiency.[3] For instance, more than 40% of the Al acceptors in *p*-type SiC epilayers are compensated.[4,5]

The two types of vacancies, the silicon-site one within the charge state q (V_{Si}^q) and the carbon-site one (V_C^q), behave in a different manner. Due to the lack of *p* electrons in the carbon core the dangling bonds around V_{Si}^q are strongly localized at the neighboring C atoms. On the other hand, considering the characteristic distances in SiC the Si-dangling bonds around V_C^q are rather extended. The distance 3.09 Å of two neighboring Si atoms is only slightly larger than their bond length of 2.35 Å in pure silicon. Therefore, like in the case of a vacancy in Si, carbon vacancies in SiC should be candidates for a symmetry-lowering distortion of the surrounding lattice in order to gain energy via formation of dimerlike bonds between neighboring Si atoms. Indeed, measurements show that the positively charged carbon vacancy V_C^+ is subject to such a Jahn-Teller distortion[2] and calculations indicate the same behavior for V_C^0.[6] Moreover, it seems that the resulting energy gain due to the Jahn-Teller effect is much larger for V_C^0 compared to V_C^+ so that a negative-*U* behavior[7] occurs.[8,9] In contrast, the single negatively charged silicon vacancy V_{Si}^- shows no symmetry lowering. The electron paramagnetic resonance (EPR) spectra of this defect are characterized by an isotropic g factor. This fact may be interpreted in two different manners:[1,10,11] (i) The V_{Si}^- vacancy is in a low-spin state ($S=1/2$, like in the case of pure silicon), and a dynamical Jahn-Teller effect gives rise to the isotropy of the g factor. (ii) The vacancy ground state is a high-spin ($S=3/2$) orbital singlet state $^4A_2$. It would demonstrate the importance of exchange interactions for V_{Si}^-, in agreement with the monovacancy in diamond.[11] Recent electron spin resonance (ESR) and electron nuclear double resonance (ENDOR) studies[2,10] favor the latter interpretation.

The understanding of the electronic structure of the vacancies is poor. Deep level transient spectroscopy (DLTS) (Ref. 12) found that a cubic SiC film is free of deep levels in the upper third of the band gap. However, other authors[13] observed two levels at 0.34 and 0.68 eV below the conduction-band minimum (CBM). Photoluminescence studies[14–16] also indicate the existence of vacancy-related deep levels in the fundamental gap. A tight-binding calculation in the framework of a one-electron theory[17,18] shows the existence of states within the band gap. Existing more sophisticated calculations in the framework of the *ab initio* density-functional theory (DFT) in the local-density approximation (LDA) do not include either spin effects[9] or the lattice relaxation[10] or both.[3]

The physical picture of the formation and properties of vacancies is complicated by the pronounced polytypism of the compound. More than 200 SiC polytypes have been determined.[19] The most extreme polytypes are zinc blende, 3C-SiC, with pure cubic stacking of the Si-C bilayers in [111] direction and wurtzite, 2H-SiC, with pure hexagonal stacking in [0001] direction. The other polytypes represent hexagonal (H) or rhombohedral (R) combinations of these stacking sequences with *n* Si-C bilayers in the primitive cell. Besides 3C-SiC the technological important polytypes are 4H- and 6H-SiC with four or six bilayers and, hence, eight or twelve atoms in the corresponding unit cell.[20]

The different stacking of the Si-C bilayers does not only remarkably influence the properties of the SiC crystals but

also those of the defects. The indirect band gap varies in a wide range from 2.4 eV (3C) to 3.3 eV (2H).[21] Consequently, the position of the vacancy levels should vary from polytype to polytype. A second problem arises from the $n/2$ inequivalent Si and C atomic sites in the hexagonal unit cells. Because of the crystal field, their positions parallel to the c axis are not fixed by the lattice constant c.[22] Moreover, the stacking gives rise to two hexagonal bilayers and $(n-2)$ cubic bilayers. Consequently, in 4H there are two inequivalent atomic sites with either hexagonal (h) or quasicubic (k) character for each atom sort.

Our aim is to study the electronic and atomic structure as well as the spin state and the energetics for monovacancies. In particular, we want to investigate whether the differently charged vacancies become important defects in SiC for certain experimental conditions characterized by the Fermi-level position (doping) and the stoichiometry (sample preparation). The electronic energy levels are derived with respect to the band edges and the orbital and spin characters of the associated system states are discussed. The influence of the polytype is also investigated. The cubic (zinc blende) 3C structure with space group T_d^2 and the hexagonal 4H crystal with space group C_{6v}^4 are considered as the prototypical SiC polytypes. For these purposes we perform *ab initio* total-energy calculations for the vacancies in different charge states and at different atomic sites. All atoms are fully relaxed and the spin-related exchange-correlation effects are also taken into account.

The paper is organized as follows. The computational method and formulas are presented in Sec. II. In Sec. III, a detailed analysis of our results is given and the different properties of the vacancies and the underlying physics are discussed. Finally, a summary is given in Sec. IV.

II. COMPUTATIONAL METHOD

A. Total energies and Kohn-Sham eigenvalues

Our calculations are based on the density functional theory (DFT) (Ref. 23) in the local density approximation (LDA) or local spin-density approximation (LSDA).[24] Only valence electrons are explicitly considered. Their interaction with the atomic cores is treated by non-normconserving *ab initio* Vanderbilt pseudopotentials.[25] They are implemented into the Vienna *ab initio* simulation package. [26,27] A slightly modified version of the Rappe-Rabe-Kaxiras-Joannopoulos scheme[26,28] is used for the construction of the pseudopotentials. In almost all cases of elements it leads to the softest possible pseudopotentials. This happens also for silicon, although it is more important for the first-row element carbon.[29] The pseudopotential scheme used allows the expansion of the single-particle wave functions into a plane-wave basis set. It is restricted by a kinetic energy cutoff of 13.2 Ry. This restriction corresponds to about 55 plane waves per atom. The pseudopotentials and the cutoffs were tested by calculating the lattice constants and bulk moduli of the SiC polytypes. The lattice constants were reproduced within 1.5% of experimental values and the bulk moduli to within 6% of the best experimental values.[29] The cubic lattice constant of 3C-SiC amounts to $a_0 = 4.332$ Å, whereas the two hexagonal lattice constants of 4H-SiC are $a = 3.061$ Å and $c = 10.013$ Å. In order to test the pseudopotentials and the plane-wave expansion further, calculations were also performed on the main bulk polytypes of silicon carbide. We found not only reasonable values for their total-energy differences but also for the extremely small internal cell relaxations.[22,30]

The exchange and correlation energy per electron is described by the quantum Monte Carlo results of Ceperley and Alder[31] in the parametrization of Perdew and Zunger.[32] In order to avoid partially errors due to the use of frozen cores nonlinear core corrections to the exchange-correlation energy[33] are included in the generation of the pseudopotentials. In the spin-polarized case the correlation energy for arbitrary polarization is determined by using the same interpolation between the nonpolarized and fully polarized case as for the exchange energy (standard interpolation.[34]) The resulting single-particle Kohn-Sham equations[24] are solved using a band-by-band residual minimization method[27]. The Kohn-Sham eigenvalues are taken to interpret the bulk band structures and the vacancy levels. They do not account for the excitation aspect and, hence, underestimate the excitation energies of the system.[35,36] The energy gaps resulting within the DFT-LDA of 1.33 eV (3C-SiC) and 2.23 eV (4H-SiC), respectively, are much smaller than the experimental values of about 2.39 and 3.27 eV at low temperatures.[21]

B. Supercells and k-space summation

In order to model the vacancies in the framework of the described pseudopotential-plane-wave method we apply a supercell method. In the case of the cubic polytype our convergence tests showed that a simple cubic (sc) supercell with 64-atomic sites is almost sufficient to describe the energetics. Nevertheless, we have done calculations for a face-centered cubic (fcc) 128-atom supercell and for a sc arrangement of 216-atom supercells. The vacancies are created by leaving one atomic site empty within one supercell. In these artificial crystals the distance of two neighboring vacancies amounts $D = 2a_0 = 8.66$ Å, $D = 2\sqrt{2}a_0 = 12.25$ Å, or $D = 3a_0 = 13.00$ Å, for the 64-atom, 128-atom, and 216-atom supercell, respectively.

In order to model the vacancies in the hexagonal 4H polytype the elementary cell of this crystal is enlarged in the directions vertical to the c axis. The primitive basis vectors are increased by a factor of 3 or 4, which results in two hexagonal supercells with 72 and 128 atoms, respectively. The creation of one vacancy on a lattice site gives rise to a vacancy-vacancy distance of $D = c = 10.01$ Å parallel to the c axis and $D = 3a = 9.18$ Å perpendicular to the c axis for the 72-atom and $D = 4a = 12.24$ Å perpendicular to the c axis for the 128-atom supercell.

The supercell approach is also used to simulate different charge states of the vacancies. In these cases electrons are removed (or added) from (to) the supercell to (from) a non-interacting reservoir level, where they do not contribute to the exchange-correlation or Hartree potential except through the zero-Fourier component of the charge density. In other words, a rigid background charge density smeared out over the entire cell is introduced in order to neutralize the supercell.

The periodic arrangement of supercells including a vacancy in sc or fcc Bravais lattices means that the wave vector

running through the Brillouin zone (BZ) of the corresponding reciprocal lattice gives a set of good quantum numbers for the characterization of the single-particle states. Important quantities such as the total energy and the electron density contain BZ summations and are performed by using a special-point technique.[37] Usually, in the cubic case, a $4\times4\times4$ mesh is used for the 64-atom, and a $2\times2\times2$ mesh for the 128-atom and 216-atom supercell arrangements. In the hexagonal case we use a $2\times2\times2$ mesh for both supercells. The results are, however, checked also for a $3\times3\times3$ **k** point set.

The supercell method introduces an artificial interaction between vacancies in adjacent supercells. This effect causes a dispersion of the defect-related energy levels in the gap.[6] Consequently, one gets defect bands rather than defect levels. Therefore, in the paper we present only results for the large 216-atom (3C) and 128-atom (4H) supercells. However, even for the largest supercells used the dispersion remains important for calculations concerning single charged vacancies (V^+ or V^-) and operating with more than one **k** point in the irreducible part of the BZ (IBZ). In these cases, due to the spin-degeneracy, the uppermost occupied (defect-related) energy band is only half filled. Therefore, vacancy states at different **k** points are not occupied uniformly, as it would be the case for the isolated vacancy. Instead, the band is only filled at **k** points where the lowest eigenvalues occur. This mechanism would favor the single charged vacancies compared to charge states with completely filled defect bands. For that reason, we introduce a constraint in the calculations with more than one **k** point to ensure the uniform occupation of the defect bands.

In order to include the spin influence the LSDA calculations are performed starting from the atomic geometries optimized within the LDA. The BZ sampling is, however, restricted to the Γ point. This is suggested by the splitting of the t_2-related defect bands due to the vacancy-vacancy interaction outside Γ, even for the cubic case and keeping the T_d symmetry. When this splitting at finite **k** points overcomes the spin-induced level splitting, the formation of high-spin vacancy states will be suppressed artificially. At Γ and keeping the local T_d symmetry the defect-related t_2-bands remain threefold degenerate (with spin sixfold) and, therefore, behave as the t_2 levels of an isolated vacancy. The exchange-correlation effects can lead to a separation of the $t_2^{\uparrow}$- and $t_2^{\downarrow}$-levels and, hence, to a preferred filling of one of the spin orbitals in dependence on the charge state of the vacancy.

C. Formation energies and charge-dependent defect levels

In the thermal equilibrium the concentrations of the vacancies V_X^q are determined by their formation energies.[38] They depend on the chemical potential μ_X of the atom $X=$C,Si, which is removed from the corresponding lattice site, and the charge state q of the generated vacancy. The chemical potential μ_X allows us to model every possible stoichiometry, more strictly the preparation conditions during the vacancy generation. The five different charge states are labeled by $q=++,+,0,-$, and $--$, i.e., $(2-q)$ defines the number of electrons occupying the t_2-derived defect bands. The lower-lying a_1 bands are always occupied with two electrons of opposite spin. The reservoir of the electrons is described by their chemical potential E_F+E_V, if the Fermi energy E_F is measured relative to the valence-band maximum (VBM) E_V.

We adapt the formalism by Zhang and Northrup.[39] At low temperatures the formation energy of a vacancy V_X^q is given by

$$\Omega_f(V_X^q,\mu_X,E_F)=E_{tot}(V_X^q)-N\mu_{SiC}^{bulk}+\mu_X+q(E_V+E_F), \tag{1}$$

where $E_{tot}(V_X^q)$ is the total energy of the defect supercell in question. The vacancy is generated in an ideal bulk system with N Si-C pairs. Their chemical potential μ_{SiC}^{bulk} is defined by the total energy of the $2N$-atom supercell divided by the number of pairs. In the thermal equilibrium it holds

$$\mu_{SiC}^{bulk}=\mu_{Si}+\mu_C. \tag{2}$$

Under extremely Si-rich or C-rich preparation conditions the chemical potentials of the individual atoms approach the corresponding bulk values, $\mu_X=\mu_X^{bulk}$ $(X=Si,C)$. Therefore, it is convenient to consider deviations $\Delta\mu_X=\mu_X-\mu_X^{bulk}$ from these values. Their allowed range is determined by the heat of formation of the SiC compound

$$\Delta H_f=\mu_{Si}^{bulk}+\mu_C^{bulk}-\mu_{SiC}^{bulk}. \tag{3}$$

The calculated chemical potentials of the pure bulk crystals of the constituents are $\mu_{Si}^{bulk}=2.38$ eV and $\mu_C^{bulk}=-1.80$ eV with respect to the value $\frac{1}{2}\mu_{SiC}^{bulk}$. The total-energy difference between diamond and graphite is small enough[29] to prevent a serious error in the formation energy of SiC. We evaluated it to be $\Delta H_f=0.58$ eV independent of the polytype.[30] This value is slightly smaller than the measured heat of formation, $\Delta H_f=0.72$ eV,[40] and a calculated number $\Delta H_f=0.75$ eV.[41] The differences indicate the uncertainties in the experimental determination and, respectively, computation of this thermochemical quantity. In accordance with the preparation conditions the fluctuations of the chemical potentials of the two constituents vary between C-rich conditions, i.e., $\Delta\mu_{Si}=-\Delta H_f$ $(\Delta\mu_C=0)$, and Si-rich conditions, i.e., $\Delta\mu_{Si}=0$ $(\Delta\mu_C=-\Delta H_f)$. For convenience we introduce the difference $\Delta\mu=\Delta\mu_{Si}-\Delta\mu_C$, which varies between $\Delta\mu=-\Delta H_f$ (C-rich) and $\Delta\mu=\Delta H_f$ (Si rich).

According to Eq. (1) the formation energy of a charged vacancy V_X^q depends on the chemical potential E_V+E_F of the electrons. Its absolute value is governed by the position of the VBM, E_V, in the defect supercell. The definition of this reservoir level is accompanied by three problems.

(i) In a supercell calculation, due to finite-size effects, the position of the VBM in the defect supercells of different charge states differs from its position in the perfect crystal. Therefore it is necessary to estimate the proper lineup of the energy levels in order to get the position of the VBM in the defect supercell. For such an alignment we use the lowest *s*-like energy level, i.e., the lowest valence band at the Γ point, because the corresponding *s*-like eigenstate should be influenced by the presence of a vacancy in a similiar manner as the averaged potential. The band structures of the defect supercells are shifted by an energy amount which brings their lowest energy levels at Γ in coincidence with that of the perfect crystal. This shift depends on the size of the supercell

and on the size of the open volume in the neighborhood of the vancant site. It is strongest for the Si vacancy in its double positively charged state and, due to the Jahn-Teller distortion, smallest for the C vacancy in its neutral charge state. However, the variation of the shift with the charge state of the vacancies is only weak (0.01 eV for V_C and 0.04 eV for V_{Si} in a sc supercell with 216 atoms), whereas the averaged total shift amounts to 0.03 eV for V_C and 0.1 eV for V_{Si}. Therefore, we have applied these averaged shifts in the explicit calculations but have neglected the fluctuations due to the charge state. We have also checked the alignment procedure according to Garcia and Northrup,[42] where the VBM value from the bulk supercell calculation is corrected by the difference between the average electrostatic potential in a bulklike environment of the defect supercell and the average potential in the ideal bulk supercell. We found a similiar alignment as described above.

(ii) The absolute value E_V can be defined in different ways. We have calculated the position of the VBM by means of the same total-energy method as used for the difference $E_{tot}(V_X^q)-N\mu_{SiC}^{bulk}$ in Eq. (1). Strictly speaking, the value E_V (E_C) is calculated within the delta self-consistent field (ΔSCF) method[43] as the difference of the total energy of the ideal supercell and that within the charge state $q=+$ ($q=-$). As expected[24,44] the resulting values are practically identical with the corresponding Kohn-Sham eigenvalues taking into account the band dispersion. In the case of the 64-atom cell, where we use four mesh points in the IBZ, we find a mean value. In the case of the 216-atom cell with only a single mesh point in the IBZ we end up with the Kohn-Sham eigenvalue at this particular **k** point.

(iii) In the chemical potential E_V+E_F in Eq. (1) the Fermi energy E_F varies in order to simulate the doping level of the crystal under consideration. For strict *p*-type conditions it holds $E_F=0$. In the case of strict *n*-type doping the chemical potential should be identified with the conduction-band minimum, E_C. In other words, it holds $E_F=E_g$ where the energy gap is given by $E_g=E_C-E_V$.

In the case of the negatively charged vacancies, which should occur in the *n*-type doping case, extra electrons are involved. We relate the total energies of the negatively charged vacancies to the corresponding value E_C. By means of relation (3) and the definition of the fluctuations of the chemical potentials the formation energy in Eq. (1) can be written as ($q=++,+,0,-,--$):

$$\Omega_f(V_X^q,\Delta\mu,E_F)=E(V_X^q)\pm\frac{1}{2}\Delta\mu+q[\Theta(q)E_F+\Theta(-q)(E_F-E_g)], \tag{4}$$

$$E(V_X^q)=E_{tot}(V_X^q)+q[\Theta(q)E_V+\Theta(-q)E_C]-\left(N-\frac{1}{2}\right)\mu_{SiC}^{bulk}\pm\frac{1}{2}(\mu_{Si}^{bulk}-\mu_C^{bulk}), \tag{5}$$

where the upper (lower) sign is valid for the Si(C) vacancies. The energy $E(V_X^q)$ is independent of $\Delta\mu$ and E_F.

Removing (or adding) an electron from (to) the supercell to (from) a reservoir level corresponds to a single-particle excitation. For that reason, the excitation aspect has to be taken into the calculation of E_g. Unfortunately, the ΔSCF method[43] does not give the correct gap energy since the corresponding Bloch states are extended over the whole supercell. Self-energy calculations[35,36] would be helpful. They are already done for different SiC polytypes.[45] Plotting the formation energies over the width of the fundamental gap, we use the experimental values $E_g=2.39$ eV (3C-SiC) and $E_g=3.26$ eV (4H-SiC).[21]

The resulting formation energy depends on the vacancy V_X^q, the preparation conditions $\Delta\mu$, and the doping level E_F. Neglecting the effects due to the formation entropy, which are small compared to Ω_f itself, the equilibrium concentration of a defect is given by $c(V_X^q)=N_s\exp(-\Omega_f/k_BT)$, where N_s is the concentration of the sublattice sites. It holds $N_s=5.0\times10^{22}$ cm^{-3} for SiC rather independent of the polytype.

The acceptorlike ionization levels $(q+1/q)$ of a vacancy are independent of the preparation conditions, i.e., the actual value of the chemical potential μ_{Si} or μ_C. They are defined as the position of the Fermi level E_F at which the charge state of the considered defect changes from $q+1$ to q.[46] Then, using Eq. (1) one has to solve $\Omega_f(V_X^{q+1},\Delta\mu,E_F)=\Omega_f(V_X^q,\Delta\mu,E_F)$ with respect to E_F. One finds for the acceptor ionization level

$$\varepsilon_A(q+1/q)=E_{tot}(V_X^{q+1})-E_{tot}(V_X^q)-E_V. \tag{6}$$

For instance, for $q=-1$ the acceptor excitation energy $\varepsilon_A(0/-)$ gives the energy that is necessary to bring a single negatively charged vacancy in its neutral charge state. Therefore, $\varepsilon_A(0/-)$ formally measures the energy to bring one electron from the vacancy into the valence bands.

Acceptor ionization levels may be traced back to donor ionization levels

$$\begin{aligned}\varepsilon_D(q-1/q)&=E_g-\varepsilon_A(q/q-1)\\&=E_C+E_{tot}(V_X^q)-E_{tot}(V_X^{q-1}),\end{aligned} \tag{7}$$

where the first number $(q-1)$ characterizes the charge state of the vacancy in the initial state and the second one after excitation of one electron into the CBM. For instance, for $q=0$ the donor excitation energy $\varepsilon_D(-/0)$ defines the energy that is needed to bring one electron from a t_2-derived vacancy level into the conduction band. Consequently, it holds $\varepsilon_D(-/0)+\varepsilon_A(0/-)=E_g$. Explicitly, in the following we use the representation:

TABLE I. Geometry and total energy of charged monovacancies V_X^q in 3C-SiC. The local symmetry, the relaxation parameters b and p_1 (in percentage of the bulk bond length, cf. Fig. 1), and the distance of two nearest-neighbor (NN) atoms of the vacancy are given. The two different values indicate the pairing mechanism. The total energy given in Eq. (5) which is independent of stoichiometry and doping is listed. Energy values in parentheses include spin-dependent exchange-correlation effects.

Vacancy	Symmetry	b (Å)	p_1 (Å)	NN distance (Å)	Total energy (eV)
V_C^{--}	D_{2d}	−0.06	0.21	2.72, 3.10	4.22 (4.22)
V_C^{-}	D_{2d}	−0.06	0.20	2.74, 3.11	4.26 (4.26)
V_C^{0}	D_{2d}	−0.05	0.20	2.75, 3.11	4.30 (4.30)
V_C^{+}	D_{2d}	0.05	0.09	3.20, 3.04	2.91 (2.89)
V_C^{++}	T_d	0.12	0.00	3.26	1.17 (1.17)
V_{Si}^{--}	T_d	0.16	0.00	3.32	6.97 (6.72)
V_{Si}^{-}	T_d	0.16	0.00	3.32	7.70 (7.17)
V_{Si}^{0}	T_d	0.17	0.00	3.34	8.69 (8.45)
V_{Si}^{+}	T_d	0.18	0.00	3.36	8.08 (8.02)
V_{Si}^{++}	T_d	0.21	0.00	3.40	7.68 (7.68)

$$\varepsilon_D(q-1/q)=\begin{cases}[E_{tot}(V_X^q)+qE_C]-[E_{tot}(V_X^{q-1})+(q-1)E_C], & q=-1,0\\ E_g+[E_{tot}(V_X^q)+qE_V]-[E_{tot}(V_X^{q-1})+(q-1)E_V], & q=+1,+2\end{cases}. \tag{8}$$

In the following we restrict ourselves to the donor excitation levels $\varepsilon_D(q-1/q)$ in Eq. (8). They may formally be interpreted in a single-particle band picture. In this picture they give the energetical distance of a certain defect level characterized by the pair $(q-1/q)$ to the CBM. The positions of these levels allow an easy characterization of the defect, in our case the vacancy, as a donor, an acceptor or none of them. One has (i) a pure donor, when the level $(q/q+1)$ lies in the gap but not $(q-1/q)$; (ii) a pure acceptor, if $(q-1/q)$ lies in the gap but not $(q/q+1)$; (iii) an amphoteric defect, i.e. the center is both a donor and an acceptor, if both levels $(q-1/q)$ and $(q/q+1)$ are found within the fundamental gap.

In the case of an amphoteric center V_X^q the energetical distance of the two levels $(q-1/q)$ and $(q/q+1)$ characterizes the interaction of the electrons occupying the t_2-derived vacancy states. Because of the localization of these states, it may be represented by an effective Coulomb integral, a so-called Hubbard energy U.[47] It holds

$$\begin{aligned}U&=\varepsilon_D(q/q+1)-\varepsilon_D(q-1/q)\\&=E_{tot}(V_X^{q+1})+E_{tot}(V_X^{q-1})-2E_{tot}(V_X^q).\end{aligned} \tag{9}$$

This definition of the Hubbard U parameter can be motivated also in another way dividing the total energy of the vacancy system approximately into a contribution of the twofold positively charged vacancy and a contribution due to the $n_q=2-q$ electrons occupying t_2-derived levels with energy $\varepsilon(n_q)$. One obtains[48]

$$\begin{aligned}E_{tot}(V_X^q)&=E_{tot}(V_X^{++})+n_q\varepsilon(n_q)-\frac{1}{2}n_q^2U,\\ \varepsilon(n_q)&=\varepsilon(0)+n_qU,\end{aligned} \tag{10}$$

where $\frac{1}{2}n_q^2U$ represents the electron-electron interaction counted twice in the band-structure energy $n_q\varepsilon(n_q)$. The single-particle vacancy level $\varepsilon(n_q)$ is also charge dependent.[49] The definitions in Eq. (10) fulfill the Janak theorem,[50] $\varepsilon(n_q)=\partial E_{tot}(V_X^q)/\partial n_q$. Replacing the terms on the right-hand side of Eq. (9) by expression (10), it follows the equality to the Hubbard U parameter.

III. RESULTS AND DISCUSSION

A. Geometry

Important results of the total-energy minimizations within 216-atom supercells are summarized in Table I for the C- and Si-site vacancies in different charge states q in 3C-SiC crystals. The data obtained with a 64-atom supercell are nearly the same. This holds particularly for the geometry parameters. The total energies may change by an amount of about 0.3 eV. In the first step spin effects are omitted and the optimizations are performed within the LDA. Within the accuracy of the determination of the minimum of the total energy and, hence, vanishing Hellmann-Feynman forces only the local symmetries D_{2d} (for V_C^q, apart from V_C^{++}) and T_d (for V_{Si}^q) occur. If local minima are found for the two other possible symmetries C_{3v} and C_{2v}, then they are higher in energy and therefore not discussed here.

In our calculations C-site vacancies in 3C-SiC do not really exist in negatively charged states. This might be due to the underestimation of the energy gap within the DFT-LDA, which prevents the occurrence of defect-related energy levels in the upper region of the fundamental gap. Instead, the excess electrons necessary to create negatively charged vacancy states occupy the lowest lying conduction-band states, i.e., we model neutral vacancies with additional electrons in the conduction band rather than negatively charged C vacan-

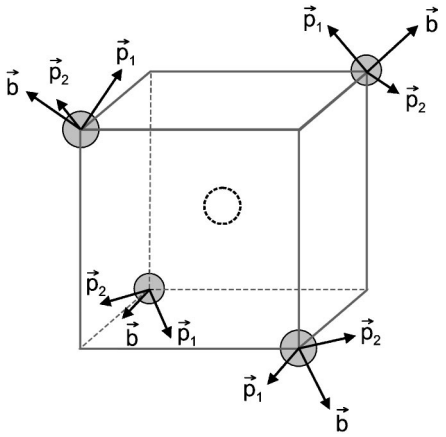

FIG. 1. Possible relaxations of the atoms 1, 2, 3, and 4 around the vacancy. **b** characterizes the outward breathing mode parallel to a body diagonal [111], $[\bar{1}\bar{1}\bar{1}]$, $[\bar{1}\bar{1}1]$, or $[1\bar{1}\bar{1}]$. The pairing mode component $\mathbf{p_1}$ is pointing along $[\bar{1}\bar{2}2]$, [112], $[1\bar{1}2]$, or $[\bar{1}\bar{1}2]$. The vectors $\mathbf{p_2}$ orthogonal to the previous two indicate a further reduction of the local symmetry.

cies. For that reason the relaxation pattern for V_C^- and V_C^{--} is nearly identical with the relaxation of V_C^0, as can be seen in Table I.

Two relaxation parameters are given in Table I. They describe the displacements of the four nearest neighbors of the vacancy (cf. Fig. 1). The parameter b characterizes the breathing mode. The atoms move towards or away from the position of the missing atom parallel to a body diagonal, keeping the local T_d symmetry unaltered. For V_C^0 this parameter is negative, indicating an inward relaxation of the neighboring Si atoms. Additionally, the system might gain energy by a symmetry-lowering pairing mode, described by the parameter p_1. Two neighboring atoms of the vacant site move towards each other in a plane parallel to one of the (001) planes and form a dimerlike bonding configuration, thereby reducing the ideal tetrahedral symmetry to a local tetragonal D_{2d} symmetry. This is exactly what happens for V_C^0. The pairing mode parameter $p_1 = 0.20$ Å is quite large. The costs in energy to distort the crystal locally are overcome by an energy gain due to the overlap of dangling bonds and formation of new dimerlike bonds.[6] The dimer bond length of 2.75 Å is remarkably shorter than the ideal second-nearest-neighbor distance of 3.06 Å in SiC and approaches the bond length of 2.35 Å in pure silicon.

If one removes an electron from V_C^0, forming a positively charged C-site vacancy V_C^+, the breathing mode changes drastically from an inward to an outward relaxation, i.e., the nearest-neighbor atoms move away from each other and the system lowers its energy by a shortening of the bonds between first- and second-nearest-neighbors of the vacancy. In addition, a pairing mode relaxation which, on the other hand, reduces the distance between the two pairs of nearest neighbors, occurs. These two tendencies result in a configuration where the paired atoms have shortened their distance by a small amount of 0.02 Å, whereas the distance to the other two atoms is increased by 0.14 Å. It shows that the system has the capability to gain energy by charge redistribution even for quite small changes in the interatomic distances, because the dangling bonds at the nearest-neighbor Si atoms seem to overlap already remarkably at distances of 3.06 Å, i.e., in the unrelaxed atom configuration.[6]

Removing another electron, changing over to the double positively charged C vacancy, the outward breathing relaxation increases and the pairing mode disappears completely. Only two electrons which occupy s-like defect states with energy levels within the valence bands are located at the vacancy. They do not force any kind of bonding, and, consequently, there are no driving forces for a symmetry-lowering pairing of atoms or another sort of Jahn-Teller distortion.

Exactly the latter mechanism dominates the atomic relaxations around the Si-site vacancy for any charge state, not only the doubly positive one as in the case of the C vacancy. Due to the strong localization of the C2s and C2p orbitals the dangling bonds located at the nearest-neighbor carbon atoms in a distance of 3.06 Å in the ideal SiC crystal cannot substantially overlap. Therefore, the only energy gain is related to a shortening of C-Si bonds between first- and second-nearest-neighbors of the vacancy, accompanied by a significant outward breathing mode. It increases with the reduction of the number of electrons from 0.16 Å (V_{Si}^{--}) to 0.21 Å (V_{Si}^{++}). Simultaneously the distance of two C neighbors of the vacancy also increases from 3.32 Å to 3.40 Å.

Summarizing the structural results, there is a pronounced Jahn-Teller effect with a symmetry reduction in the case of the neutral carbon vacancy V_C^0. The effect is weakened for V_C^+ and vanishes for V_C^{++}. In our calculations the carbon vacancy does not exist in negatively charged states. For silicon vacancies no Jahn-Teller distortion occurs independent of their charge state. The T_d symmetry is conserved and the basic mechanism is an outward breathing relaxation which increases with decreasing number of electrons located at the Si vacancy.

B. Energetics

According to the definition in Eq. (5) the total energies $E(V_X^q)$ in Table I are given with respect to the bulk conduction-band edge E_C or valence-band edge E_V in dependence on the charge state of the vacancy in 3C-SiC. They are independent of stoichiometry and doping and define the Hubbard energy U according to Eq. (9). For the Si vacancies one estimates the values $U = 0.21$ and 0.26 eV (without spin-dependent exchange-correlation effects) for the positively or negatively charged systems, i.e., a weakly repulsive electron-electron or hole-hole interaction. The situation changes drastically for the positively charged carbon vacancies. One finds a negative-U behavior with $U = E_{tot}(V_C^{++}) + E_{tot}(V_C^0) - 2E_{tot}(V_C^+) = -0.35$ eV. The situation is similar to that in pure silicon. There, a strong negative-U behavior is predicted[51] and observed[52] for positive monovacancies. It is mainly due to the strong Jahn-Teller distortion in the case of the neutral vacancy.[9] The pairing of the neighboring Si atoms lowers the total energy significantly. As a consequence, the effective electron-electron interaction appears to be attractive.

The relation

$$E_{tot}(V_C^{++}) + E_{tot}(V_C^0) < 2E_{tot}(V_C^+) \qquad (11)$$

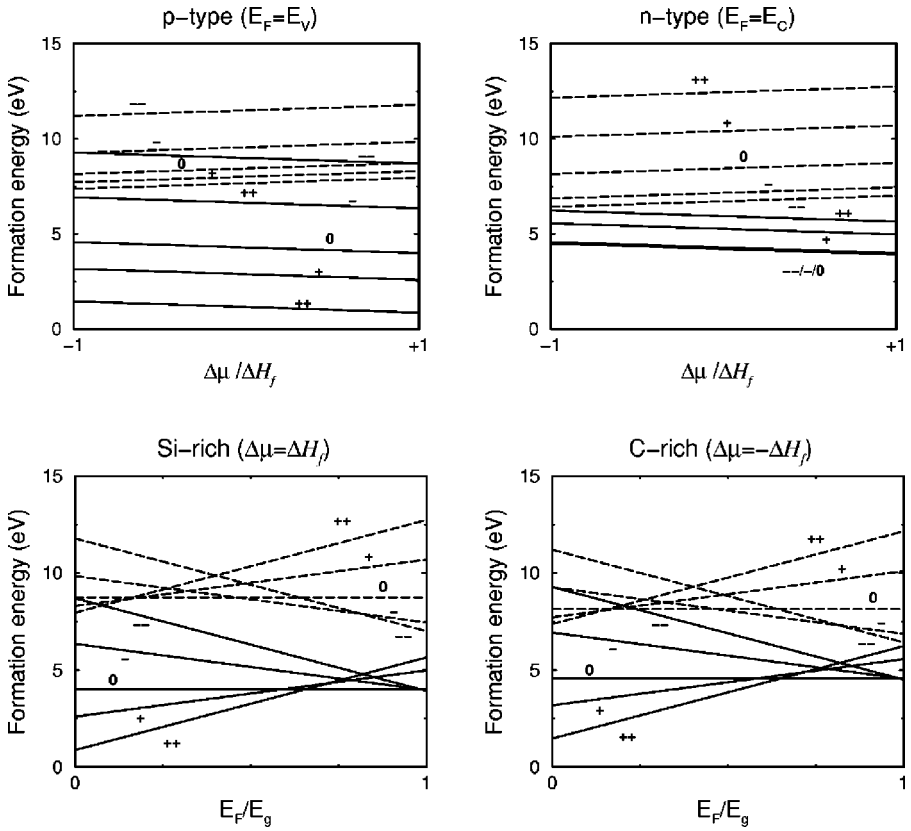

FIG. 2. Formation energy of C (solid line) and Si (dashed line) vacancies in 3C-SiC as a function of the preparation conditions (difference $\Delta\mu$ of the chemical potentials) and the Fermi-level position E_F.

implies that the V_C^+ carbon vacancy is metastable. The reaction $2V_C^+ \rightarrow V_C^0 + V_C^{++}$ gives rise to a lowering of the system energy. Nevertheless, single positively charged C vacancies have been observed by means of ESR for *p*-type 3C-SiC irradiated with protons.[2] The D_{2d} symmetry and the low-spin state agree with our predictions. We trace back the experimental observation of V_C^+ to the situation of the irradiated crystal far from thermodynamic equilibrium. The electron transfer between two V_C^+ vacancies is prevented. This interpretation is supported by annealing experiments. The defect center disappears above a temperature of 100 °C and about 80% of the initial amount is lost after 200 °C annealing[2].

The calculated vacancy formation energies for the different charge states of C-site and Si-site vacancies are shown in Fig. 2, resulting within the 216-atom cell and DFT-LDA calculations. The electron chemical potential E_F is tuned from the VBM ($E_F=0$) to the CBM ($E_F=E_g$), where the experimental value is used for E_g. The preparation conditions are described by a variation of the difference of the fluctuations $\Delta\mu=\Delta\mu_{Si}-\Delta\mu_C$ of the chemical potentials of the constituents. Figure 2 clearly indicates the favorization of the occurrence of the carbon vacancies versus the silicon vacancies under equilibrium conditions. Only under extremely C-rich preparation conditions and high *n*-doping levels the formation energy of V_{Si}^{--} approaches the values for C vacancies. The reason for this behavior is not essentially related to the vacancy itself. In any case four Si-C bonds have to be broken during the vacancy creation. Rather, the energy gain to bring the atom (occuping the vacancy site before the defect creation) into the reservoir with the corresponding chemical potential is generally higher in the carbon case.

Under equilibrium conditions, in the *p*-type limit the carbon vacancy is a double donor, regardless of stoichiometry. For moderate *n* doping the neutral C-site vacancy is the most favorable one. Whether or not negatively charged states may occur for *n* doping cannot be clearly answered by our calculations. The favorization of the double positively charged carbon vacancy V_C^{++} in a wide range of doping levels agrees with results of previous pseudopotential-plane-wave calculations[3] but contradicts the findings from non-self-consistent calculations.[53] It may explain why ''as-grown'' cubic SiC is always weakly *n* type as well as the lowered doping efficiency of acceptors.[2,4,5] 40–60 % of Al acceptors are compensated in *p*-type epilayers.[5]

C. Electronic structure

The differences of the total energies given in Table I determine the ionization energies of the vacancies. The results obtained according to Eq. (8) are represented in Table II and in the level schemes of Fig. 3. The resulting level schemes of the C and Si vacancy appear essentially within the fundamental gap closer to either the conduction-band edge or the valence-band edge. The position of the two term schemes in the fundamental gap reflects the energetical ordering of Si- and C-hybrid energies, since the Si- or C-dangling hybrids basically form the defect states of the C-site or Si-site vacancy. The center of gravity of the level scheme of the Si

TABLE II. Ionization energies (in eV) of C and Si vacancies in 3C-SiC with respect to the VBM. Unstable levels are indicated by parentheses.

	C vacancy		Si vacancy		
Level	LDA	LSDA	LDA	LSDA	Ref. 10
$(+/++)$	1.74	1.72	0.41	0.34	0.42
$(0/+)$	1.39	1.41	0.61	0.43	0.54
$(-/0)$	(2.35)	(2.35)	1.39	1.11	1.06
$(--/-)$	(2.35)	(2.35)	1.65	1.94	1.96

vacancy 1.02 eV above the VBM is closer to the valence bands. Nevertheless, it represents an amphoteric defect and not a pure acceptor.

The situation is different in the case of the C-site vacancy. The center of gravity of the level scheme (without the negative charge states) 0.83 eV below the CBM indicates a more donorlike character. The occurrence of the $(--/-)$ level in the conduction bands corresponds to the fact that the twofold negatively charged C vacancy cannot exist. The extra electron is immediately donated into a conduction-band state or, in other words, it remains localized at a shallow donor in the crystal. The second interesting fact concerns the level ordering. Whereas the term scheme of the t_2-related charge-dependent defect levels of the Si vacancy exhibits the usual ordering, the donor level $\varepsilon_D(0/+)$ lies below the donor level $\varepsilon_D(+/++)$ in the carbon case. The reason is the same as mentioned during the discussion of the metastability of V_C^+. According to Eq. (9) it seems that the effective Coulomb energy U would be negative (with a value $U=-0.35$ eV) instead of positive. When the chemical potential E_F of the electrons is raised, there is a transition from V_C^{++} to V_C^0 because the energy gained by the stronger distortion due to the second electron occupying a t_2-derived level overcomes the Coulomb repulsion of adding the second electron.

The principal findings of Fig. 3 are also reflected within a single-particle picture (cf. Fig. 4) constructed from the Kohn-Sham eigenvalues of the DFT-LDA in a 64-atom supercell. The fundamental gap at Γ in the projected bulk band structure (shaded region) represents the Kohn-Sham gap $E_g=1.32$ eV. The defect bands (solid lines) have been identified by studying the wave-function squares of the supercell bands along the ΓX direction. The lower a_1-derived band lies deep in the valence bands independent of the chemical

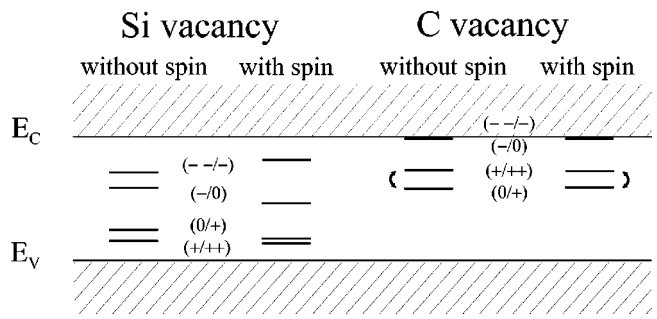

FIG. 3. Energy-level scheme for the silicon and carbon vacancy centers in 3C-SiC. Energy levels shown result from LDA or LSDA calculations within the 216-atom supercell approach.

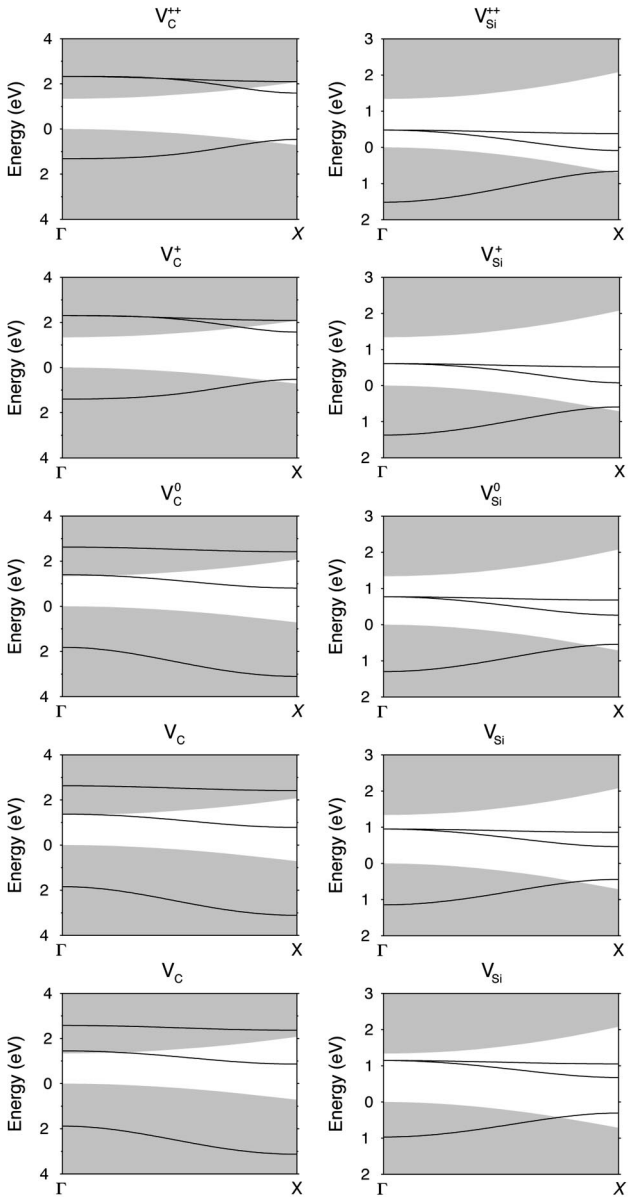

FIG. 4. Band structures of the sc supercell arrangements of 64 (63)-atom cells versus the high-symmetry line ΓX in the little Brillouin Zone (BZ) for C and Si vacancies. The projected bulk bands are indicated as shaded regions. The solid lines indicate the calculated vacancy bands with b_2-, e-, and a_1-like (D_{2d} symmetry) or t_2- and a_1-like (T_d symmetry) character.

nature of the vacancy. It is therefore always occupied with two electrons. Because of the vacancy-vacancy interaction it shows a substantial upward (T_d symmetry) or downward (D_{2d} symmetry) dispersion along ΓX. The t_2-related bands possess a dispersion with lower energies at X in comparison to the values at Γ. In the T_d case they are threefold degenerate at Γ. The corresponding splitting Δ_{JT} of the bands into b_2- and e-like bands characterizes the strength of the Jahn-Teller distortion, i.e., the pairing mechanism in the D_{2d} case.

In the Si case the t_2-related bands are located within the fundamental gap (cf. Fig. 4). For the **k** point set used in the structural optimization the occupation of the bands is correct. For the V_C^q vacancies the situation is more difficult since the t_2-derived defect bands show a tendency to approach or to lie

TABLE III. Defect level energies and Jahn-Teller splittings derived from a fit of the DFT-LDA bands according to Ref. 6. Bands obtained for 64-atom supercells have been used. All values are in units of eV. The VBM represents the energy zero.

Vacancy	ε_{a_1}	ε_{t_2}	Δ_{JT}
V_C^{--}	−3.88	1.61	1.04
V_C^{-}	−3.88	1.61	1.16
V_C^{0}	−3.88	1.62	1.13
V_C^{+}	−0.08	1.73	0.00
V_C^{++}	−0.04	1.73	0.00
V_{Si}^{--}	0.03	0.82	0.00
V_{Si}^{-}	−0.09	0.62	0.00
V_{Si}^{0}	−0.17	0.43	0.00
V_{Si}^{+}	−0.20	0.25	0.00
V_{Si}^{++}	−0.24	0.10	0.00

in the conduction bands. The application of the procedure of Ref. 6 to fit the DFT-LDA defect bands to analytical expressions obtained within a nearest-neighbor vacancy tight-binding picture gives formally rise to the level energies ε_{a_1} and ε_{t_2} (T_d case) as well as the Jahn-Teller splitted levels $\varepsilon_e=\varepsilon_{t_2}+(1/3)\Delta_{JT}$ and $\varepsilon_{t_2}=\varepsilon_{t_2}-(2/3)\Delta_{JT}$ (D_{2d} case). The corresponding values are listed in Table III. In the Si case there is a moderate dependence on the charge state. In the average it holds $\varepsilon_{t_2}=0.33E_g$ and $\varepsilon_{a_1}=-0.12E_g$. For the C vacancies one observes a drastic change with the symmetry lowering. Whereas the center of gravity of the t_2-derived states is with $\varepsilon_{t_2}=1.27E_g$ more or less conserved the a_1-level moves from $\varepsilon_{a_1}=-0.05E_g$ to $\varepsilon_{a_1}=-2.94E_g$ accompanied by a remarkable Jahn-Teller splitting $\Delta_{JT}=0.84E_g$. The results for the t_2 levels agree with results of simplified tight-binding calculations[17] or linear-muffin-tin orbital (LMTO) treatments[18] for the neutral vacancies. The values of these calculations are $\varepsilon_{t_2}=0.23$ or $0.14E_g$ (V_{Si}^0) and $\varepsilon_{t_2}=0.69$ or $0.68E_g$ (V_C^0).

The DFT-LDA band structures shown in Fig. 4 for the carbon vacancies also make obvious several problems of the supercell approach. They are formally indicated by the occurrence of defect bands within the conduction bands for the carbon vacancy. As already mentioned, the lowest conduction-band states are occupied instead of defect-related bands for V_C^- and V_C^{--}. This is also the reason why the ionization levels $(-/0)$ and $(--/-)$ lie more or less exactly on the conduction-band minimum (Fig. 3). Another serious problem is related to the dispersion of the highest occupied defect band in the V_C^+ case. In a 64-atom supercell this band overlaps partly with the conduction bands due to the vacancy-vacancy interaction. As a consequence, depending on the **k** point, the occupation of the states could be wrong, especially near the Γ point. Therefore it is necessary to enlarge the supercell in order, on the one hand, to reduce the interaction, and on the other hand, to reduce the number of **k** points. The latter point makes it easier to guarantee the correct occupation of defect levels. A combination of a treatment in a 216-atom supercell and the use of only one special **k** point, which results from a $(2\times2\times2)$ Monkhorst-Pack mesh, fulfills these criteria, although the situation of the band overlap in the V_C^+ case remains critical. However, checking the orbital character of the highest occupied states at the single **k** point, we find that for V_C^+ indeed localized defect states (corresponding to the lower t_2-derived band) are occupied and no extended conduction-band states. Hence, we really describe the ground state of the V_C^+ vacancy and, therefore, the negative-U behavior of the carbon vacancy. This effect is stabilized with increasing size of the supercell used. For a 64-atom supercell the U value is only -0.30 eV, compared to -0.35 eV in the 216-atom cell. That means that the negative-U behavior is more pronounced for larger supercells. Therefore, we claim that the prediction of the negative-U behavior of the positively charged carbon vacancy is correct.

D. High-spin states

Table I clearly shows that within the LDA the driving forces for a Jahn-Teller distortion are not significant in the case of the Si vacancy. The local T_d symmetry is conserved within the accuracy of our calculations and the ground state of the Si-site vacancies should be degenerate apart from the double positively charged one. This is an important argument against, e.g., a one-electron configuration $a_1^2t_2^{\uparrow\downarrow}$ of the V_{Si}^0 defect. In order to investigate the spin influence on the defect formation we perform calculations also within the framework of the LSDA. We start from the geometries optimized within the LDA. The spin-dependent exchange-correlation (XC) effects are studied by adding the total-energy differences between LSDA and LDA, calculated by taking into account only the Γ point in the **k**-space sampling, to the LDA results. According to Fig. 4 only at the Γ point the t_2-derived bands simulate the orbital degeneracy being typical for t_2 levels of a defect with spatial T_d symmetry. Otherwise the explicit consideration of the band splitting due to the vacancy-vacancy interaction would prevent the formation of high-spin states as an artifact of the supercell approach. The total defect energies with spin-dependent XC effects are also listed in Table I.

In the case of the carbon vacancies the spin effects are negligible. For V_C^{++}, V_C^0, and V_C^{--} the total spin S of the system is zero; a situation which we correctly describe within the LDA. In the case of V_C^+ with a total spin $S=1/2$ the energy lowering is small with 0.02 eV. The situation is similar for the defects V_{Si}^{++} ($S=0$) and V_{Si}^{+} ($S=\frac{1}{2}$) with energy lowerings of 0.00 and 0.07 eV for the ground states $^1A_1$ or $^2T_2$. However, the picture is completely changed for the neutral and negatively charged Si-site vacancies. According to Hund's rule high-spin states appear. The ground states are $^3T_1$ ($S=1,V_{Si}^0$), $^4A_2$ ($S=\frac{3}{2},V_{Si}^-$), and $^3T_1$ ($S=1,V_{Si}^{--}$)[54] with energy lowerings ΔE of 0.24, 0.53 or 0.25 eV. The XC effects lower the energy approximately according to the relation $\Delta E\approx0.24\ \mathrm{eV}\times S^2$.

The mechanism of gaining energy is accompanied by a strong XC splitting of the $t_2^{\uparrow}$- and $t_2^{\downarrow}$ levels and, hence, with a filling of the energetically lower lying spin orbitals, e.g., the spin-up orbitals. These splittings of the t_2-level amount 0.26 (V_{Si}^+), 0.49 (V_{Si}^0), 0.72 (V_{Si}^-), and 0.54 (V_{Si}^{--}) eV. The resulting one-electron configurations are $a_1^2t_2^{\uparrow\uparrow}$ (V_{Si}^0), $a_1^2t_2^{\uparrow\uparrow\uparrow}$ (V_{Si}^-), and $a_1^2t_2^{\uparrow\uparrow\uparrow}t_2^{\downarrow}$ (V_{Si}^{--}), maximizing the effective spin in

agreement with Hund's rule. Due to the four C-dangling bonds surrounding a Si-site vacancy the situation is similar to that for the monovacancies in diamond. This concerns the outward relaxation and the conservation of the local T_d symmetry,[55–57] but also the formation of the high-spin states.[55] The findings that the high-spin configurations are stable are in complete agreement with another DFT-LSDA calculation using the LMTO method to calculate the electronic structure.[10] Also ESR spectroscopy[2] clearly indicates the existence of the V_{Si}^{-} center in a $S=3/2$ state and in an environment with T_d symmetry.

The influence of the spin-dependent XC effects on the defect ionization levels is represented in Fig. 3 and Table II. The effect is small for the C vacancies. Also the negative-U behavior is only weakly influenced. The most important changes happen for the Si-site vacancy. The splitting of the two levels $(-/0)$ and $(--/-)$ is symmetrically enlarged, whereas the splitting of the levels $(+/++)$ and $(0/+)$ is slightly decreased. The resulting energy levels are in reliable agreement with the calculations of Wimbauer *et al.*[10]. The different positions of the levels $(+/++)$ and $(0/+)$ found to be closer to the VBM in our calculations is a consequence of the structural optimization missing in Ref. 10. Our results are slightly in contrast to other *ab initio* calculations using 128-atom supercells.[58] Torpo *et al.* find larger distances of the $(+/++)$ and $(0/+)$ levels with respect to the VBM.

E. Influence of crystal structure

The most striking differences between the hexagonal polytypes nH and the zinc-blende one 3C concern the increase of the number of atoms in the supercell by a factor n and the change of the space-group symmetry from T_d^2 to C_{6v}^4. They arise from the change of the stacking sequence ABC (3C) to $ABCB$ (e.g., 4H) as indicated in Fig. 5. We restrict the consideration of the hexagonal polytypes to the 4H one. It is the hexagonal polytype with the smallest unit cell that contains inequivalent atomic sites with either cubic (k) or hexagonal (h) character. The tetrahedrons around these lattice sites are differently deformed. Hence, the dangling bonds localized at each atom and contributing to the bonding are not anymore completely sp^3 hybrids.

Three important consequences occur for the vacancies in 4H in comparison to 3C.

(i) There exist two inequivalent carbon and silicon vacancies in accordance to the two inequivalent sites h (atoms 1 or $1'$ in Fig. 5) or k (atom 2 or $2'$ in Fig. 5), from which an atom may be removed.

(ii) The inequivalence of the dangling bonds surrounding a vacancy gives rise to a splitting of the t_2-vacancy level which is threefold degenerate in 3C already without structural relaxations. In other words, the local point-group symmetry is already reduced to C_{3v} in comparison to T_d (ideal vacancies in 3C-SiC). The structural optimizations of the total energy are therefore performed without a symmetry restriction.

(iii) The change of the stacking sequence results in an increase of the fundamental energy gap by about 1 eV from 3C to 4H. This remarkable change in the electronic structure will influence the energetical stability and the ionization levels of the vacancies. No problems concerning the occupation

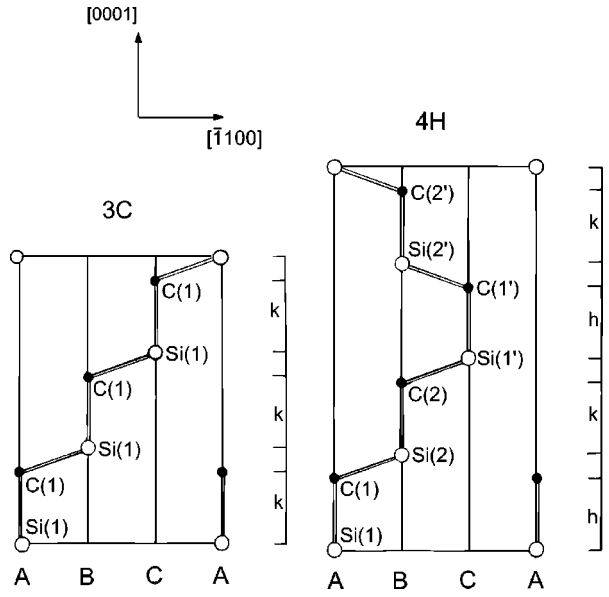

FIG. 5. The zig-zag chain structure of the cubic (3C) and a hexagonal (4H) SiC polytype. The atomic positions are indicated in the $(11\bar{2}0)$ plane. The different $(\bar{1}100)$ planes within the hexagonal unit cells are denoted by *A*, *B*, and *C*. The cubic (k) or hexagonal (h) character of Si-C bilayers in the [0001] direction is given according to the parallel (k) or nonparallel (h) limiting bonds.

of the higher single-particle vacancy levels occur in contrast to the 3C case, i.e., also the negatively charged C vacancies exist in 4H-SiC.

Results of the total-energy minimizations within the DFT-LDA (cf. Table IV) are presented in Fig. 6 for the formation energies of C and Si vacancies in 4H-SiC at inequivalent lattice sites and in different charge states. They are very similar to those already discussed in the case of the cubic polytype. The variations are of the order of 0.1 eV. They arise mainly from the change of the unit cell and the **k**-point set and, therefore, cannot be fully traced back to the change of the stacking sequence of the Si-C bilayers along the c axis. Only the differences between cubic and hexagonal sites of maximum values of about 0.12 eV (V_C^0) and 0.20 eV (V_{Si}^{++}) are real consequences of the stacking. The larger changes in the total energies, and formation energies of V_X^{-} and V_X^{--} follow from the higher excitation energies for electrons. The energies are lowered by about 0.8 eV $(X=\mathrm{C})$ and 1.8 eV $(X=\mathrm{Si})$ per electron in the average mainly as a consequence of the increase of the gap in 4H. This fact makes the occupation of defect levels in the fundamental gap by electrons more likely. The different energies per electron reflect the fact that the Si vacancy levels are closer to the VBM than the C-related ones. Consequently the energy gain is larger for $X=\mathrm{Si}$. Figure 6 clearly indicates that in the thermodynamic equilibrium the formation of the vacancies hardly depends on the cubic or hexagonal character of the corresponding atomic site. The site-induced variations are small compared to the formation energy itself. Generally, it holds that the formation of a C (Si) vacancy is slightly favored on a cubic (hexagonal) lattice site. Only the V_{Si}^{--} defect deviates from this rule.

The interpretation of the atomic relaxations around the vacancies is rather complicated due to the wide loss of local

TABLE IV. Geometrical changes around a vacancy V_X^q at a cubic (k) or hexagonal (h) lattice site in 4H-SiC for the three inequivalent nearest-neighbor atoms (in percentage of the bulk bond length). The total energy of the 128-atom supercell is calculated as in LDA and LSDA (in parentheses).

Vacancy	Site	b^1 (%)	b^2 (%)	b^3 (%)	p_1^1 (%)	p_1^2 (%)	p_1^3 (%)	Total energy (eV)
V_C^{--}	k	−3.0	−30.5−	-3.5	7.7	0.8	8.6	2.68 (2.68)
	h	−3.0	−30.4	−1.9	9.1	1.6	5.8	2.74 (2.74)
V_C^-	k	−1.8	−15.5	−4.4	1.2	8.5	11.7	3.57 (3.50)
	h	−8.8	−2.4	−1.5	11.1	2.7	3.7	3.67 (3.59)
V_C^0	k	−2.5	−4.5	−3.0	9.7	10.9	11.7	4.03 (4.03)
	h	−2.7	−5.0	−2.5	10.5	9.8	10.1	4.15 (4.15)
V_C^+	k	2.5	1.4	2.3	3.8	4.3	4.5	2.71 (2.65)
	h	2.7	0.5	3.0	3.9	2.9	4.2	2.77 (2.71)
V_C^{++}	k	6.0	6.0	7.5	0.0	0.0	0.0	0.98 (0.98)
	h	5.9	5.9	6.1	0.0	0.0	0.0	1.03 (1.03)
V_{Si}^{--}	k	9.9	9.9	8.0	-0.5	-0.5	0.0	4.87 (4.63)
	h	8.3	8.3	7.6	0.4	0.4	0.0	4.92 (4.66)
V_{Si}^-	k	9.8	9.8	8.1	-0.2	-0.2	0.0	6.45 (5.96)
	h	8.8	8.8	7.7	0.4	0.4	0.0	6.43 (5.98)
V_{Si}^0	k	10.3	10.3	8.1	0.4	0.4	0.0	8.31 (8.05)
	h	9.6	9.6	8.0	0.8	0.8	0.0	8.23 (7.97)
V_{Si}^+	k	10.6	10.6	9.8	0.4	0.4	0.0	7.94 (7.84)
	h	10.5	10.5	9.2	0.6	0.6	0.0	7.81 (7.66)
V_{Si}^{++}	k	10.9	10.9	13.5	-0.2	-0.2	0.0	7.78 (7.78)
	h	11.5	11.5	10.5	0.3	0.3	0.0	7.58 (7.58)

symmetry, particularly in the case of the C-site vacancies. Nevertheless, even in the case of carbon vacancies one point-group symmetry operation survives as a consequence of the superposition of the C_{3v} crystal symmetry and the local D_{2d} defect symmetry known from the C-site vacancies in 3C-SiC. The resulting symmetry group is C_{1h}, consisting of one mirror plane and the identity operation. As a consequence two of the three nearest-neighbor atoms in a plane perpendicular to the c axis remain equivalent. Hence, the displacements of three inequivalent nearest-neighbor atoms have to be studied. The geometrical relaxation of each of these inequivalent atoms ($i=1,2,3$) is, as in the 3C case, characterized by an individual breathing and pairing parameter (cf. Fig. 1, but transformed into hexagonal coordinates). The small deformations of the tetrahedrons in the defect-free 4H-SiC lattice[22,30] are neglected. In Table IV three breathing mode parameters b^i and also three pairing mode parameters p_1^i are listed. In each case the first parameter represents the two nearest-neighbor atoms of the vacancy which are equivalent due to the mirror plane. The remaining two nearest-neighbor atoms lie within the mirror plane and have their own parameters each. We identify the third atom as that above the vacancy in the c-axis direction. As in the case of 3C-SiC there is no necessity to introduce the second pairing mode parameter p_2. The relaxation pattern of vacancies in 4H-SiC resembles the one in 3C-SiC. In the charge state $++$ no driving forces for a symmetry reduction exist and the C_{3v} symmetry is conserved. This also holds for Si-site vacancies in the other possible charge states, at least within the accuracy of our calculations. The principal outward breathing mechanism is conserved. The pairing-mode parameters are almost zero and the three breathing parameters b^1, b^2, and b^3 vary only weakly with the nearest-neighbor atom.

For V_C^+ and V_C^0 a Jahn-Teller distortion occurs. The underlying local symmetry group is indeed C_{1h}. But the diplacements of the nearest-neighbor atoms are similiar to the corresponding values of C-site vacancies in 3C-SiC (cf. Table I). V_C^0 exhibits a pronounced pairing mechanism independent of the cubic or hexagonal character of the lattice site, and the transition from the outward-breathing to the inward-breathing mode occurs changing from V_C^+ to V_C^0. In the case of V_C^- and V_C^{--} the relaxation behavior changes drastically. If these charge states would exist in 3C-SiC a further symmetry reduction would be necessary to lift the remaining degeneracy of the D_{2d} ground state. For example, an additional symmetry reduction from D_{2d} to C_{2v} could be expected. This is qualitatively what happens in 4H-SiC in the case of a single negatively charged C vacancy. The symmetry of the resulting local geometry is quite similiar to a C_{2v} symmetry in a distorted cubic lattice. The geometrical situation is the same as for D_{2d} symmetry in the case of V_C^0, except that the additional electron of V_C^- strengthens one of the two dimerlike bonds between the paired nearest-neighbor atoms. The shorter bond length is about 2.6 Å, the longer one about 2.9 Å.

The double negatively charged C vacancies show a completely different behavior. Their relaxation pattern resembles more a local C_{3v} symmetry. One of the four nearest neighbors of the vacancy shows an extremely large displacement towards the vacancy site of about 30% of the bond length. The distance to the other three nearest-neighbor atoms is with about 2.5 Å even shorter than the bond length of about 2.8 Å of the paired atoms in V_C^0 and comparable to the distance of the stronger paired atoms in V_C^-. For a cubic lattice like 3C-SiC this behavior would be understandable if

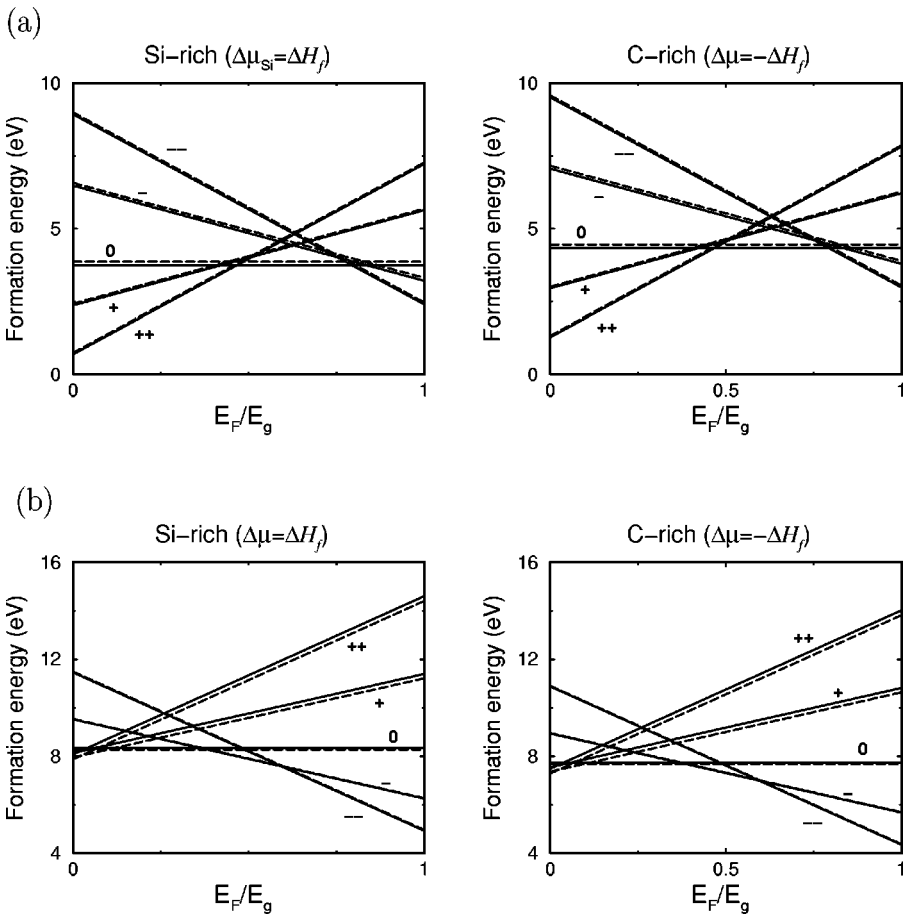

FIG. 6. Formation energy of C (a) and Si (b) vacancies in 4H-SiC as a function of the Fermi-level position E_F for the two extreme preparation conditions $\Delta\mu=\Delta H_f$ and $\Delta\mu=-\Delta H_f$. Solid line: cubic site vacancy, dashed line: hexagonal site vacancy.

one takes into account that the degeneracy of the ground state of a double negatively charged C vacancy could be already lifted by a symmetry reduction from T_d to C_{3v}. In this case the former threefold degenerated t_2 level splits into a nondegenerate a_1 and a twofold degenerate e level. In such a configuration it is possible to create a nondegenerate ground state if the twofold degenerate e level is completely occupied and the a_1 level remains unoccupied, i.e., if the e level lies energetically below the a_1 level.

The spin effect is also represented in Table IV. We observe the same situation as in the cubic case. The total spins for the charge states $q=+$, and $++$ are $S(V_X^+)=1/2$, and $S(V_X^{++})=0$ independent of the chemical and structural character of the considered lattice site. Drastic differences between C and Si vacancies occur for the neutral and negative charge states. It holds $S(V_C^0)=0$, $S(V_C^-)=1/2$, and $S(V_C^{--})=0$ due to the formation of dimerlike bonds, whereas the corresponding total spins in the Si case are $S(V_{Si}^0)=1$, $S(V_{Si}^-)=3/2$, and $S(V_{Si}^{--})=1$, i.e., the energy gain due to spin-dependent exchange and correlation dominates this kind of vacancies and forces the formation of high-spin states. Jahn-Teller distortions and accompanying symmetry reductions are a consequence of the energy gain due to the formation of bondlike structures. An energy gain due to the spin-dependent exchange, on the other hand, forces the creation of a geometry with a symmetry as high as possible. This behavior can be observed if one compares atomic displacements calculated in DFT-LDA and DFT-LSDA. In the latter case one finds a local geometry around the vacancy which is somewhat more T_d-like as in DFT-LDA. Using EPR and ENDOR such a high-spin state has been observed for the single negatively charged Si vacancy in neutron-irradiated 4H-SiC.[10] The magnetic resonance parameters of V_{Si}^- are found to be almost identical for the polytypes 3C, 4H, and 6H. This fact supports our hypothesis that the local environments of this Si vacancy are rather similar and nearly represent the T_d symmetry as in the cubic polytype.

The ionization energies of the C and Si vacancies in 4H-SiC are listed in Table V. Results obtained within LDA and LSDA are given. Figure 7 shows the resulting energy-level scheme. The dependence on the cubic or hexagonal character

TABLE V. Ionization energies (in eV) of C and Si vacancies at cubic (first value) and hexagonal (second value) sites in 4H-SiC with respect to the valence band maximum.

	C vacancy		Si vacancy	
Level	LDA	LSDA	LDA	LSDA
$(+/++)$	1.73, 1.74	1.68, 1.68	0.17, 0.23	0.06, 0.08
$(0/+)$	1.32, 1.38	1.37, 1.44	0.36, 0.42	0.20, 0.31
$(-/0)$	2.81, 2.78	2.74, 2.71	1.41, 1.47	1.19, 1.28
$(--/-)$	2.38, 2.35	2.45, 2.42	1.69, 1.76	1.94, 1.95

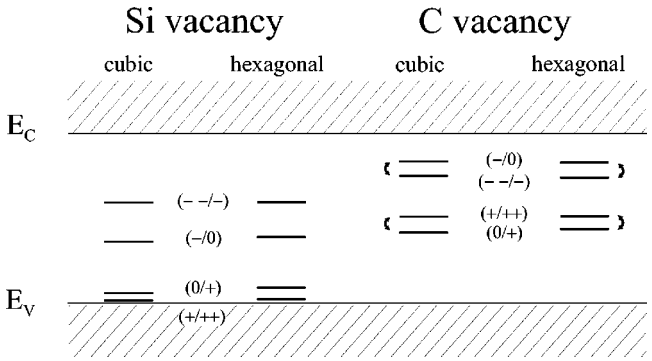

FIG. 7. Energy-level schemes for Si and C vacancies at cubic and hexagonal sites in 4H-SiC. Results are obtained from LSDA calculations within a 128-atom supercell approach.

of the site is weak. Nevertheless, a unique tendency is observed for Si-site vacancies. On average the ionization levels of the vacancies at hexagonal sites are shifted by about 0.06 eV (in LDA) towards the conduction-band edge. The C vacancy in 4H-SiC exhibits a similar negative-U behavior as found for the cubic polytype, not only for positively charged C vacancies but also for negatively charged ones. Within the LDA the normal energetical ordering of the levels $(+/++)$ and $(0/+)$ as well as $(-/0)$ and $(--/-)$ is interchanged. One derives the parameters $U=-0.41$ (-0.36) eV for the positively charged vacancies at a cubic (hexagonal) site or $U=-0.43$ (-0.45) eV for the negatively charged vacancies at a cubic (hexagonal) site. After inclusion of the spin the tendency of a negative-U behavior is somewhat reduced to $U=-0.29$ (-0.24) eV and $U=-0.29$ (-0.29) eV , respectively, but remains significant.

Despite the different crystal structures of 3C and 4H and, hence, the presence of a crystal-field splitting of the single-particle vacancy levels and the much larger energy gap in the 4H case, the level schemes in Figs. 3 and 7 (Tables II and V) are not very different, apart from the ionization levels $(-/0)$ and $(--/-)$ of the carbon vacancies, which probably do not exist in 3C-SiC. In comparison to the 3C case the levels in 4H-SiC are hardly shifted. Their energetical positions with respect to the VBM are more or less the same. Only the lowest V_{Si} levels are lower in energy by about 0.1 eV. It seems that these excitation levels follow the Langer-Heinrich rule.[59] The alignment of such deep levels of the same nature within the fundamental gap of two semiconductors determines the valence-band discontinuity between the semiconductors. The application of this rule to the situation of the lowest vacancy levels in 3C- and 4H-SiC would explain the almost vanishing valence-band discontinuity with a tendency that the VBM in 3C is lower than in 4H and the fact that the entire gap discontinuity appears as the band offset for the conduction bands.[30,45]

Experimental data about the vacancy levels are rare and, moreover, concern more or less irradiated samples. DLTS represents one sort of experiments. In the case of n-type 4H two defect levels have been observed that may be related to carbon vacancies. Deep in the fundamental gap at $E_C-1.49$ eV (Ref. 60) or $E_C-1.65$ eV (Ref. 61) a level is observed associated with a capture cross section of 10^{-14} or 2×10^{-13} cm^2. The corresponding defects are stable until annealing temperatures of 800–1300 K or at least 1000 K. They remain neutral or single negatively charged. This fact seems to indicate an identification as $(-/0)$ or $(0/+)$ level, in reasonable agreement with the level positions in Table V. A similar behavior with respect to annealing and charging has been observed for electron-irradiated p-type 4H samples.[62] Levels at $E_V+0.87$ eV and $E_V+1.30$ eV with associated cross sections 7×10^{-16} or 3×10^{-15} cm^2 have been derived. The lower level could be related to $(-/0)$ of the Si vacancy, whereas the level higher in energy could be identified with one of the lower C vacancy levels. The concentration of the defect related to the higher level increases with annealing temperature until 1300 K. Above 1600 K both defects cannot longer be detected. However, the identification of the levels observed within DLTS is complicated[63] and, because of missing additional information, highly speculative.

Another indication for vacancy levels may be found in photoluminescence spectra. For instance, after fast-neutron irradiation and subsequent thermal annealing at 1200 K (Ref. 64) the polytypes show a strongly luminescent (D_1) center. In electron-irradiated 3C-SiC it is accompanied by a zero-phonon E line, both lines slightly below 2 eV (Ref. 2). With rising hexagonality of the polytype the D_1 line is shifted to higher energies in agreement with the corresponding gap opening. In electron-irradiated 4H samples Sörman *et al.*[16] observed two sharp zero-phonon luminescence lines at photon energies of 1.35 and 1.44 eV. Because of the results of optically detected magnetic resonance instead of ''the ODMR'' measurements they argued that these lines originate from an internal transition of the neutral silicon vacancy, at least a silicon vacancy with an even number of electrons in order to explain the high-spin state $S=1$. The occurrence of two different lines in 4H is related to the two different inequivalent lattice sites for the generation of a Si vacancy. A similar explanation is given for the sharp zero-phonon line at 3.15 eV of the vacancy-related luminescence in diamond.[65] Breuer and Briddon[55] interpret it as a transition between a $^4T_1$ excited state into a $^4A_2$ ground state of the V_C^- vacancy with the single-electron configurations $a_1^{\uparrow}t_2^{\uparrow\uparrow\uparrow}$ and $a_1^2t_2^{\uparrow\uparrow\uparrow}$. Following this picture, the observations of Sörman *et al.*[16] should be related to a transition either $a_1^{\downarrow}t_2^{\uparrow\uparrow\uparrow}\rightarrow a_1^2t_2^{\uparrow\uparrow}$ or $a_1^{\uparrow}t_2^{\uparrow\uparrow\uparrow\downarrow\downarrow}\rightarrow a_1^2t_2^{\uparrow\uparrow\uparrow\downarrow}$. Unfortunately, the excited vacancy states cannot be easily calculated in our DFT-LDA ground-state theory using plane waves and supercells. However, the observed photon energies are plausible considering our results. The observed transition energies are smaller than the ionization energies of $(-/0)$ or $(--/-)$ of the Si vacancy in Table V, which may be interpreted as the energies for electron transitions from the conduction band into defect states. According to the energy values ε_{a_1} and ε_{t_2} in Table III we find in the single-particle picture excitation energies of 0.79 eV ($V_{Si}^{-\,-}$) or 0.60 eV (V_{Si}^0). Considering electron repulsion effects and the polytype influence, transition energies of 1 eV or more are not unlikely.

IV. SUMMARY

Within the DFT-LDA and, respectively, DFT-LSDA we have performed *first-principles* calculations to study possible structures, spin states, and accompanying electronic levels of

the monovacancies in different SiC polytypes. More in detail, we studied the local symmetry and the atomic displacements around the vacancy in dependence on the charge state of a vacancy with a certain chemical origin and at inequivalent lattice sites in the case of the hexagonal (4H) polytype. The energetics of the defect formation has been discussed versus the crystal doping and the preparation conditions. Ionization energies of vacancies have been studied in dependence on the number of electrons occupying the defect levels. The total spin of these electrons followed from the minimization of the total energy with respect to the electron densities related to the two different spin projections.

In the cubic case we observed a tendency for pairing of two Si atoms neighboring the C vacancy site. If more than two electrons occupy the defect states, it gives rise to the local D_{2d} symmetry. On the other hand, the atoms around the Si vacancy keep the T_d symmetry. The mechanism of the reconstruction around the vacancy is governed by an inward breathing and a pairing for the neutral C vacancy. Negatively charged C vacancies seem not to exist in 3C-SiC. A hint for this conclusion is the appearance of the levels $(-/0)$ and $(--/-)$ in 4H-SiC. They lie with about 2.4 and 2.7 eV (in LSDA) above the experimental value of 2.39 eV for the energy gap in 3C-SiC. For V_C^{++} and the Si vacancies an outward breathing reconstruction mechanism dominates. In other words, whereas the C vacancy exhibits a significant Jahn-Teller distortion, such a symmetry lowering is absent in the case of the Si vacancy. Practically, the twofold positively charged C vacancy is the most favored one for a wide range of semiconductor doping independent of the preparation conditions. Only for Fermi levels close to the conduction-band minimum (n-type doping) the neutral or the twofold negatively charged vacancies are favored in the thermodynamic equilibrium. The formation energies approach small values of about 1 eV in the limit of strong p doping and increase to values slightly below 5 eV. In principle, this picture is conserved for the 4H polytypes. There are slight variations with the inequivalent lattice sites in cubiclike or hexagonal bilayers in the unit cell. The most important changes are related to the enlargement of the fundamental energy gap by about 1 eV. As a consequence, for instance, the neutral and the twofold negatively charged C vacancy are now favored in a wider range of doping levels.

The ionization levels of the Si vacancy are close to the valence-band maximum. In the case of the C vacancy these levels are higher in energy and approach the conduction-band minimum (3C) or, in the average, midgap positions (4H). They follow the trend defined by the energetical positions of the hybrid energies of the surrounding atoms. The normal energetical ordering of the two ionization levels $(+/++)$ and $(0/+)$ of the C vacancy is destroyed for both polytypes 3C and 4H, and the same holds for the levels $(-/0)$ and $(--/-)$ in 4H. The fact that the level $(+/++)$ lies above $(0/+)$ and $(-/0)$ above $(--/-)$ can be interpreted as a negative-U behavior of the carbon vacancy. It is mainly a consequence of the remarkable energy gain accompanying the strong Jahn-Teller distortion in the V_C^0 case. The absence of such distortions in the case of the Si vacancies drives another mechanism in order to avoid a degenerate ground state. The arrangement of the electron spins for V_{Si}^{--}, V_{Si}^{-}, and V_{Si}^{0} follows Hund's rule. High-spin states give rise to the lowest total energies. The maximum total spin $S=3/2$ in the V_{Si}^{-} case is in agreement with experimental observations.

ACKNOWLEDGMENTS

Discussions with N. Achtziger, P. Deák, H. Helbig, and J. Neugebauer are gratefully acknowledged. This work was financially supported by the Deutsche Forschungsgemeinschaft (Sonderforschungsbereich 196, Project No. A8).

[1] H. Itoh, M. Yoshikawa, I. Nashiyama, S. Misawa, H. Okumura, and S. Yoshida, IEEE Trans. Nucl. Sci. **37**, 1732 (1990).
[2] H. Itoh, A. Kawasuso, T. Ohshima, M. Yoshikawa, I. Nashiyama, S. Tanigawa, S. Misawa, H. Okumura, and S. Yoshida, Phys. Status Solidi A **162**, 173 (1997).
[3] C. Wang, J. Bernholc, and R. F. Davis, Phys. Rev. B **38**, 12 752 (1988).
[4] H. J. Kim and R. F. Davis, J. Electrochem. Soc. **133**, 2350 (1986).
[5] M. Yamanaka, H. Daimon, E. Sakuma, S. Misawa, and S. Yoshida, J. Appl. Phys. **61**, 599 (1987).
[6] A. Zywietz, J. Furthmüller, and F. Bechstedt, Phys. Status Solidi B **210**, 13 (1998).
[7] G. A. Baraff, E. O. Kane, and M. Schlüter, Phys. Rev. Lett. **43**, 956 (1979).
[8] P. Deak, A. Gali, J. Miro, R. Guiterrez, A. Sieck, and T. Frauenheim, Mater. Sci. Forum **264–268**, 279 (1998).
[9] F. Bechstedt, A. Zywietz, and J. Furthmüller, Europhys. Lett. **44**, 309 (1998).
[10] T. Wimbauer, B. K. Meyer, A. Hofstaetter, A. Scharmann, and H. Overhof, Phys. Rev. B **56**, 7384 (1997).
[11] J. Schneider and K. Maier, Physica B **185**, 199 (1993).
[12] V. Nagesh, J. W. Farmer, R. F. Davis, and H. S. Kong, Appl. Phys. Lett. **50**, 1138 (1987).
[13] P. Zhou, M. C. Spencer, G. L. Harris, and K. Fekade, Appl. Phys. Lett. **50**, 1384 (1987).
[14] J. A. Freitas and S. C. Bishop, Appl. Phys. Lett. **55**, 2757 (1986).
[15] N. T. Son, E. Sörman, W. M. Chen, M. Singh, C. Hallin, O. Kordina, B. Monemar, E. Janzén, and J. L. Lindström, J. Appl. Phys. **79**, 3784 (1996); Phys. Rev. B **55**, 2863 (1997).
[16] E. Sörman, W. M. Chen, N. T. Son, C. Hallin, J. L. Lindström, B. Monemar, and E. Janzén, Mater. Sci. Forum **264–268**, 473 (1998).
[17] D. N. Talwar and Z. C. Feng, Phys. Rev. B **44**, 3191 (1991).
[18] L. Wenchang, Z. Kaiming, and X. Xide, J. Phys.: Condens. Matter **5**, 891 (1993).
[19] N. W. Jepps and T. F. Page, Prog. Cryst. Growth Charact. **7**, 259 (1983).
[20] P. Käckell, B. Wenzien, and F. Bechstedt, Phys. Rev. B **50**, 17 037 (1994).
[21] W. J. Choyke, D. R. Hamilton, and L. Patrick, Phys. Rev. **133**, A1163 (1964).
[22] A. Bauer, J. Kräußlich, L. Dressler, P. Kuschnerus, J. Wolf, K.

Goetz, P. Käckell, J. Furthmüller, and F. Bechstedt, Phys. Rev. B **57**, 2647 (1998).
[23] P. Hohenberg and W. Kohn, Phys. Rev. **136**, B864 (1964).
[24] W. Kohn and L. J. Sham, Phys. Rev. **140**, A1133 (1965).
[25] D. Vanderbilt, Phys. Rev. B **41**, 7892 (1990).
[26] G. Kresse and J. Hafner, Phys. Rev. B **47**, 558 (1993); J Phys.: Condens. Matter **6**, 8245 (1994).
[27] G. Kresse and J. Furthmüller, Comput. Mater. Sci. **6**, 15 (1996); Phys. Rev. B **54**, 11 169 (1996).
[28] A. M. Rappe, K. M. Rabe, E. Kaxiras, and J. B. Joannopoulos, Phys. Rev. B **41**, 1227 (1990).
[29] J. Furthmüller, P. Käckell, F. Bechstedt, and G. Kresse (unpublished).
[30] F. Bechstedt, A. Zywietz, K. Karch, B. Adolph, K. Tenelsen, and J. Furthmüller, Phys. Status Solidi B **202**, 35 (1997).
[31] D. M. Ceperley and B. I. Alder, Phys. Rev. Lett. **45**, 566 (1980).
[32] J. P. Perdew and A. Zunger, Phys. Rev. B **23**, 5048 (1981).
[33] S. G. Louie, S. Froyen, and M. L. Cohen, Phys. Rev. B **26**, 1738 (1982).
[34] U. von Barth and L. Hedin, J. Phys. C **5**, 1629 (1972).
[35] F. Bechstedt, Solid State Phys. **32**, 161 (1992).
[36] M. S. Hybertsen and S. G. Louie, Phys. Rev. B **34**, 5390 (1986).
[37] H. J. Monkhorst and J. D. Pack, Phys. Rev. B **13**, 5188 (1976).
[38] J. Bourgoin and M. Lannoo, *Point Defects in Semiconductors* (Springer-Verlag, Berlin, 1983), Vol. I, Chap. 6.
[39] S. B. Zhang and J. E. Northrup, Phys. Rev. Lett. **67**, 2339 (1991).
[40] O. Kubaschewski and C.B. Alcock, *Metallurgical Thermochemistry* (Pergamon, Oxford, 1979).
[41] J. E. Northrup and J. Neugebauer, Phys. Rev. B **52**, R17 001 (1995).
[42] A. Garcia and J. E. Northrup, Phys. Rev. Lett. **74**, 1131 (1995).
[43] L. Hedin and S. Lundqvist, Solid State Phys. **23**, 1 (1969).
[44] C. O. Almbladh and U. von Barth, Phys. Rev. B **31**, 3231 (1985).
[45] B. Wenzien, P. Käckell, F. Bechstedt, and G. Cappellini, Phys. Rev. B **52**, 10 897 (1995).
[46] R. Enderlein and N.J.M. Horing, *Fundamentals of Semiconductor Physics and Devices* (World Scientific, Singapore, 1997).
[47] G. D. Mahan, *Many-Particle Physics* (Plenum Press, New York, 1990).
[48] F. Bechstedt, D. Reichardt, and R. Enderlein, Phys. Status Solidi B **131**, 643 (1985).
[49] J. C. Slater, *The Self-Consistent Field for Molecules and Solids* (McGraw-Hill, New York, 1974).
[50] J. F. Janak, Phys. Rev. B **18**, 7165 (1978).
[51] G. A. Baraff, E. O. Kane, and M. Schlüter, Phys. Rev. B **21**, 5662 (1980).
[52] G. D. Watkins and J. R. Troxell, Phys. Rev. Lett. **44**, 593 (1980).
[53] P. Deak, A. Galli, J. Miro, R. Guiterrez, A. Sieck, and T. Frauenheim, Mater. Sci. Forum **258–163**, 739 (1997).
[54] F. P. Larkins and A. M. Stoneham, J. Phys. C **3**, L112 (1970).
[55] S. J. Breuer and P. R. Briddon, Phys. Rev. B **51**, 6984 (1995).
[56] D. P. Joubert, L. Li, and J. E. Lowther, Solid State Commun. **100**, 561 (1996).
[57] A. Zywietz, J. Furthmüller, and F. Bechstedt, Mater. Sci. Forum **258–263**, 231 (1997).
[58] L. Torpo, S. Pöykkö, and R. M. Nieminen, Phys. Rev. B **57**, 6243 (1998).
[59] J. M. Langer and H. Heinrich, Phys. Rev. Lett. **55**, 1414 (1985).
[60] T. Dalibor, G. Pensl, T. Kimoto, H. Matsunami, S. Sridhara, R. P. Devaty, and W. J. Choyke, Diamond Relat. Mater. **6**, 1333 (1996).
[61] C. G. Hemmingsson, N. T. Son, O. Kordina, J. L. Lindström, and E. Janzen, Mater. Sci. Eng., B **46**, 33 (1997); Mater. Sci. Forum **264–268**, 561 (1998).
[62] F. Günther, Diploma thesis, Friedrich-Schiller-Universität Jena, 1998.
[63] T. Dalibor, G. Pensl, H. Matsunami, T. Kimoto, W. J. Choyke, A. Schöner, and N. Nordell, Phys. Status Solidi A **162**, 199 (1997).
[64] V. V. Makarov, Fiz. Tverd. Tela (Leningrad) **13**, 2357 (1972) [Sov. Phys. Solid State **13**, 1974 (1972)].
[65] G. Davies, S. C. Lawson, A. T. Collins, A. Mainwood, and S. J. Sharp, Phys. Rev. B **46**, 13 157 (1992).